Taking into account the forming process in fatigue design computations

Matteo Luca FACCHINETTI[a], Bastien WEBER[b], Cédric DOUDARD[c], Sylvain CALLOCH[c]

[a] PSA Peugeot Citroën, Z.A. Louis Breguet, 78140 Vélizy-Villacoublay, France
[b] ARCELOR MITTAL, voie Romaine, 57283 Maizières-les-Metz, France
[c] Laboratoire de Mécanique des Structures Navales, rue François Verny, 29806 Brest, France

Abstract Fatigue design of mechanical parts may be based on ideal ones, without taking into account for their real geometry (e.g. thickness), the formed material state (e.g. plastic strain and residual stress) and considering fatigue data involving pre-formed materials (e.g. Wöhler curve on laminated steel sheet, instead of finished stamped parts). This approach is pragmatic, but in some cases may lead to uneffective design: failure is expected when it is not supposed to occur and damage is not predicted when it seriously affects the part. In this communication we address some ways in order to properly take into account the forming process of a mechanical part, i.e. a stamped one, in its fatigue design computation. The separate and combined effect of thickness variation, plastic strain and residual stress is considered. Numerical details are provided and physical analysis is performed.

1 INTRODUCTION

Mass reduction in automotive manufacturing is a prior objective as it straightforward leads to increase fuel efficiency, reduce emissions and a general economy in the use of material and energy resources. Thus, any improvement reducing the gap between numerical simulations and reality is supposed to lead to further design optimization.

In this framework, CAE tools have been providing effective coupled FE computation of forming-stage and service-stage for several years (see [3] for instance), even if some details of this "global approach" are still under discussion, e.g. data mapping from the forming mesh to the fatigue one, data transfer between different solvers, the choice of material hardening models, … : thus, several hypothesis are simply accepted "as-is".

Actually, due to simultaneous engineering approach and the development time reduction imposed by shorter time-to-market requirements, complete FE forming computations are usually provided when the design of the part is almost fixed, i.e. too late to feed effective design iterations. Moreover, complete and extensive material data on pre-formed material are not yet available. Definitely, there is a need for a relevant but easier fatigue design approach, based on rules coming from essential data and implying a deeper comprehension of the phenomena.

Thus, this work aims to highlight the contribution of every ingredient included in fatigue design computations when taking into account for the forming process (i.e. stamping) and identify their sensitiveness on fatigue life assessment.

This paper focuses on the design of a heavy duty, high safety grade stamped part like a suspension arm (section 2). The coupling between the forming process and the design procedure is explored from two complementary points of view: a "global approach" (section 3), concerning coupled FE computations of the forming process and the service load and a "local approach" (section 4), based on the elastic-plastic behaviour of a steel sheet subject to elementary deformations and loads. Finally, discussion and conclusions are provided (section 5).

This study is an ongoing joint project by PSA Peugeot Citroën, ARCELOR MITTAL and ENSIETA. It does not pretend to be conclusive, but traces the state-of-the-art on this subject and highlights the main questions to address and answer.

2 SUSPENSION ARM

2.1 Geometry

Let us consider the suspension arm of a pseudo Mac-Pherson front axle, as shown in figure 1: this mechanical part is fastened to the engine cradle at points E1 and E2 by means of elastic bushings and to the knuckle at point D through a ball joint.

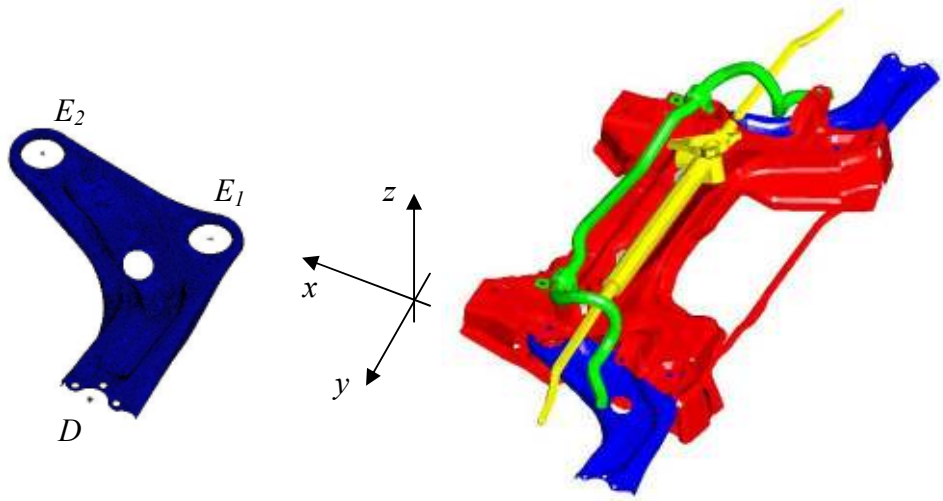

Figure 1. Front axle with engine cradle and suspension arm: notation and reference frame.

2.2 Material

The suspension arm is stamped from a 3.50 mm thick sheet steel (S 460 MC referring to EN standards). The material is assumed to be homogeneous and isotropic, with elastic-plastic behaviour and isotropic hardening. According to standard steel data and specifications on S 460 MC steel, we consider the Young modulus E = 210 GPa , the Poisson coefficient ν = 0.3 and the plasticity tangent modulus E_t = 0.84 GPa. Minimum guaranteed yield stress and limit stress are $\sigma_y = R_{p0.2}$ = 460 MPa and R_m = 520 MPa respectively, while the minimum ultimate strain is A% = 14%.

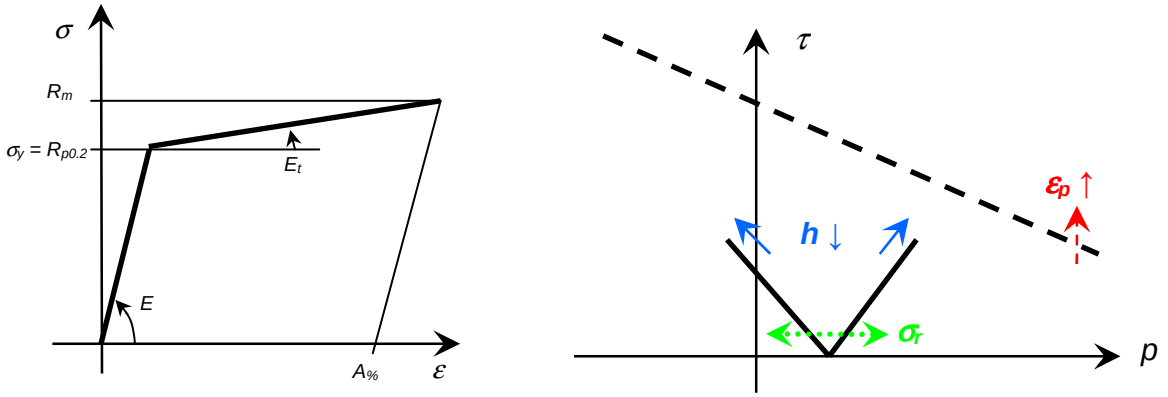

Figure 2. Steel constitutive law model (left), influence of the forming process in the Dang Van diagram (right).

More and more published work is available on the effect of pre-strain on the fatigue behaviour of steel sheets [2,5,6,8,9]. The relation between the fatigue limit (infinite lifetime) and the work hardening may be written in the form:

$$\frac{\sigma_\infty}{\sigma_{\infty 0}} = 1 + A\,\varepsilon_p \qquad (1)$$

where σ_∞ is the formed material fatigue limit, $\sigma_{\infty 0}$ is the unformed material fatigue limit, ε_p is the Von Mises equivalent plastic strain and A a constant depending on the material and the load case. A usually ranges from 1.0 up to 4.0 , so that 1% equivalent plastic strain leads to at least 1% fatigue limit increase. For the S 460 MC suspension arm steel we consider A = 1.0 [7,9].

3 GLOBAL APPROACH

In this section the coupling between the forming process and the design procedure is explored by means of FE computations of the entire mechanical part.

3.1 Stamping process

The suspension arm is formed in a two steps process on a simple effect stamping machine, under a total load from 150 to 200 kN and considering standard lubrication conditions. The part is not submitted to any thermal treatment after the forming process and standard painting process does not imply any relevant thermal cycle.

Stamping process is computed from the flat sheet to the final part, the spring-back being considered as the initial step of the fatigue design computation. FE computations are made with the commercial solver PAM-STAMP [16] using linear shell elements involving reduced integration with hourglass control, five integration points within the thickness. Such an element has a characteristic length of about 1mm and is suitable for large strains and double curvature.

As the deformed stamped mesh does not verify mesh criteria for proper fatigue computations, stamping process results (i.e. thickness scalar field, stress and strain tensor fields) are supposed to be remapped onto a more regular mesh. Considering the same stamping process data and a common regular mesh to be used for fatigue design computations, two different procedures have been tested in order to evaluate the intrinsic accuracy of the remapping procedure.

In figure 3 we show two scalar fields: on the left side the local thickness, which varies from 2.70 mm to 3.80 mm, which means that the thickness variation ranges from a reduction of 23% to an increase of 9%; on the right side the Von Mises equivalent plastic deformation on the membrane layer, which locally exceeds 25%.

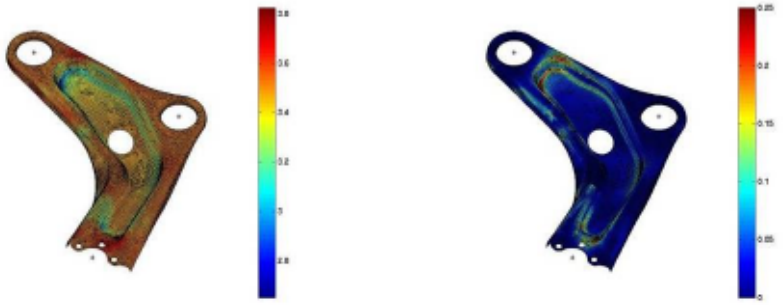

Figure 3. Stamping simulation of the suspension arm:
thickness [mm] (left), Von Mises membrane equivalent plastic strain [mm/mm] (right).

In figure 4 we highlight the difference between two independent remapping procedures: on the left side the local thickness may differ up to 0.1mm, say 3% of the initial sheet thickness; on the right side Von Mises equivalent plastic deformation on the membrane layer may be shifted up to 2%.

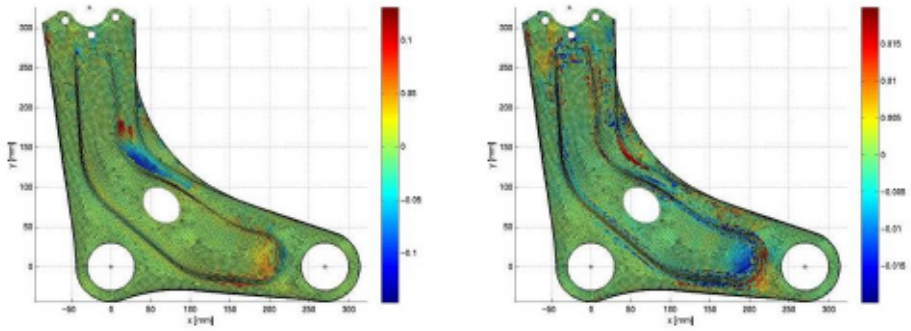

Figure 4.Differences between two independent remapping procedures: thickness [mm] (left), Von Mises membrane equivalent plastic strain [mm/mm] (right).

3.2 Fatigue design

Let us consider the high cycle fatigue regime (i.e. failure expected between 10^5 and 10^7 cycles), where the initiation crack phase is known to be dominant in the total fatigue life. Within this framework, we apply the macro-meso approach introduced by Dang Van [1] and developed by Papadopoulos [4], for which the cumulated plastic strain at a mesoscopic scale is considered as the damage variable.

The fatigue design load case is described in figure 5: a cyclic sinusoidal force of amplitude F and a loading ratio R=-1 is applied at the point D in the longitudinal x axis; boundary conditions are defined as follows: E_1 is a perfect ball joint, E_2 is constrained in y and z axes, D is constrained in z direction.

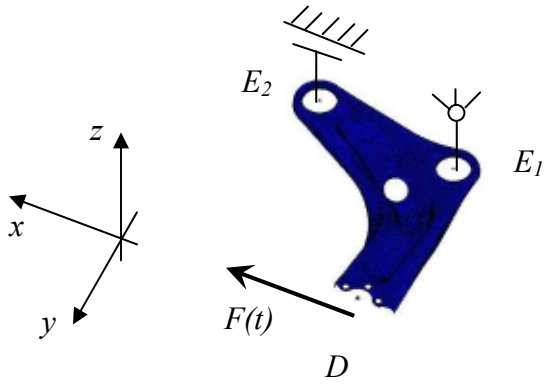

Figure 5. Fatigue design load case: applied force and boundary conditions.

FE computations are made with the commercial solver ABAQUS [14] using linear shell elements involving reduced integration and three integration points within the thickness. Such an element has a characteristic length of about 5mm. Prior to any fatigue computation, it is necessary to evaluate the asymptotic response of the structure under the defined cyclic loading: this imply to compute the spring-back and then verify the elastic shakedown. Finally, fatigue life estimations based on Dang Van approach are computed by the commercial software nCode Design Life [15]. Figure 6 shows results performed on the top surface of the suspension arm (i.e. visible upper face in figure 5). The stabilized residual stress field is obtained after only five loading cycles and associated to a final plastic strain field (fig 6.a and fig 6.b). FEA are applied on the sole geometry considering the thickness variations issued from stamping (fig 6.c and fig 6.d) or the constant nominal thickness (h_0 = 3.50 mm) of the flat products (fig 6.e and fig 6.f). The considered unit loadings are divided for positive and negative load (+F and -F) in order to take into account the geometrical non-linearity.

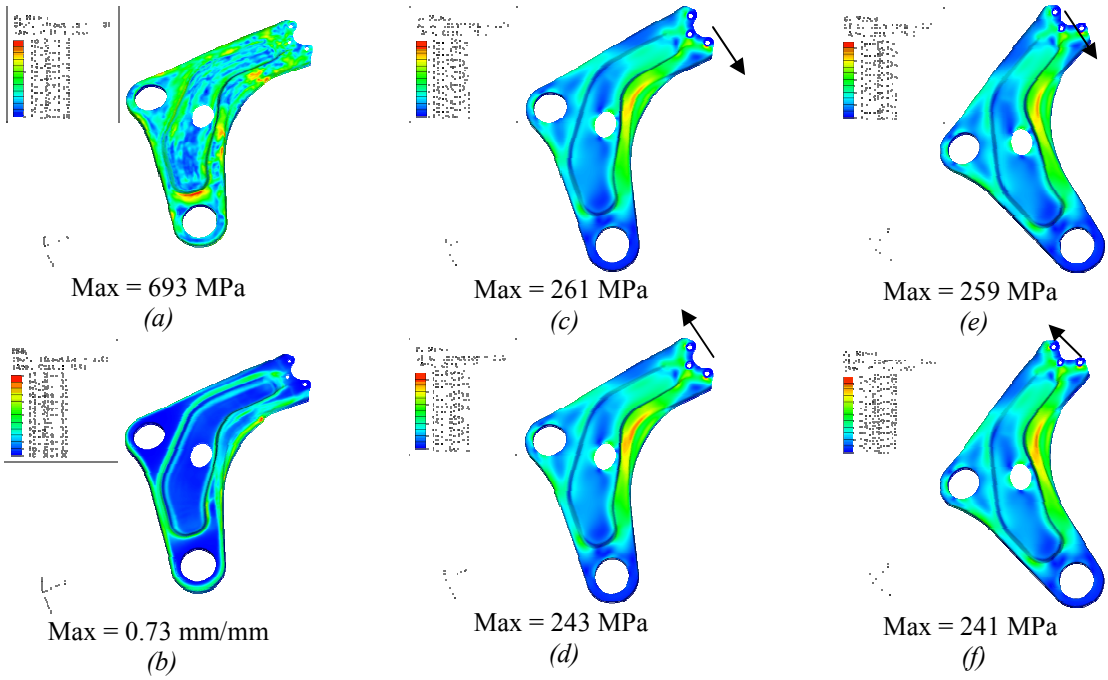

Figure 6. FEA results: Von-Mises stabilized residual stresses (a), plastic strain distribution (b), Von-Mises stress for positive (c) and negative (d) loads with thickness variations, Von-Mises stress for positive (e) and negative (f) loads with constant thickness.

Four fatigue computations have been performed on the top surface of the suspension arm in order to compare the contribution of the investigated parameters in the fatigue design modelling:

1. *initial modelling*. Nominal thickness h_0 = 3.50 mm is considered and the constant fatigue properties are those of the base metal, i.e. reference Dang Van parameters $\tau = \tau_0$ and $\alpha = \alpha_0$
2. *effect of the thinning*. The thickness distribution computed form the stamping simulation is introduced, whereas the fatigue properties are those of the base metal
3. *effect of the plastic strain* (partial coupling). The thickness distribution is introduced and the fatigue properties are updated by the local plastic strain, element by element, from zero strain up to the maximal strain, as formulated by equation (1). Dang Van parameters are then $\tau = (1+A\varepsilon_{eq})\tau_0$ and $\alpha = \alpha_0$
4. *forming and spring-back effects*, adding residual stresses (full coupling). The thickness distribution is introduced, the fatigue properties are updated by the local plastic strain as in the previous point and finally the stabilized residual stresses are superposed to the fatigue load cases as a "mean stress effect".

These four fatigue modelling proposals, from the simplest one to the most achieved, were easily supported by the last nCode Design Life software oriented to fatigue design [15], allowing a rapid comparison of their results. For all computations the focus area is the central part of the arm where a global bending occurs. The iso-values of the Dang Van Safety Factor (DV SF) are shown in the following table, ranging between the local minimal value and a factor 10 (central column), and between the local minimal value and a factor 2 by pointing on the weakest element (right column).

fatigue design / parameters	*DV Safety Factor [local min,10]*	*DV Safety Factor [local min,2]*
1-constant nominal thickness and base metal fatigue properties. *Minimal DV SF = 1.156 (reference)* *Element number = 40263*	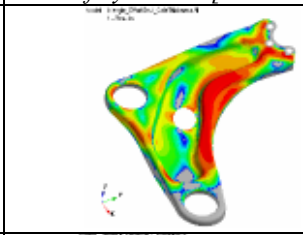	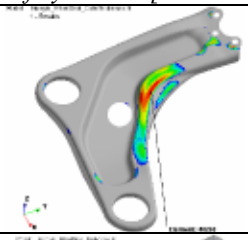
2-variable thickness from forming and base metal fatigue properties. *Minimal DV SF = 1.143 (-1.12%)* *Element number = 40263*	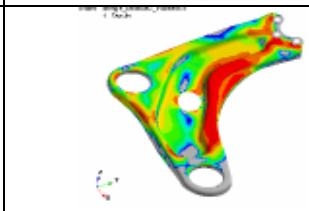	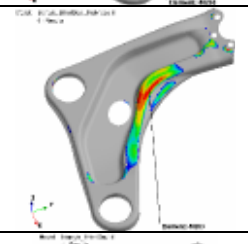
3-variable thickness and fatigue properties locally updated with plastic strain. *Minimal DV SF = 1.223 (+5.80%)* *Element number = 40263*	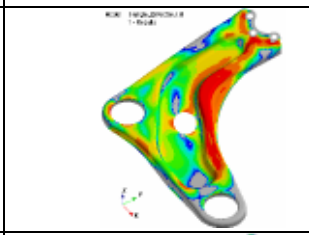	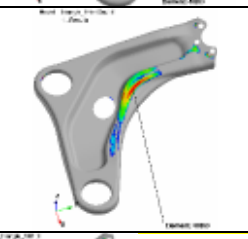
4-variable thickness, fatigue properties locally updated with plastic strain and stabilized residual stress. *Minimal DV SF = 0.981 (-15.14%)* *Element number = 40339*	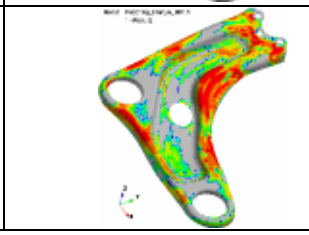	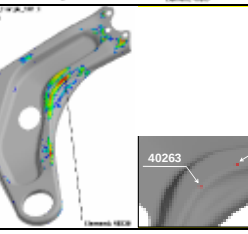

Looking at the safety factor field, cases 1 to 3 lead to almost the same damage distribution and the same critical value location. Compared to the first uncoupled computation (reference), thinning obviously implies a reduction of the safety factor (-1.12%), whereas the hardening contributes much more positively to fatigue strength (+5.80%). Nevertheless, the last fully coupled fatigue computation shows a very new damage distribution and actually is the less conservative one (-15.14%): compared to other cases, some damaged regions disappear and some others become almost critical. This is emphasised by a new location of the critical value, not so close to the initial position.

All these numerical results show the interest to properly include the forming process and its issues (thickness, residual stresses and hardening) in fatigue design, in order to reduce the gap between the fatigue safety factor measured by experimental test and that obtained by computation. However, any modelling assumption and any approximation must be criticized to assess the relevance of the entire FEA.

4 LOCAL APPROACH

In this section the coupling between the forming process and the design procedure is addressed by considering the elastic-plastic behaviour of a thin steel sheet undergoing elementary deformations (see figure 7). We establish analytical relations between the geometry of the deformed sheet, i.e. its thickness variation h / h_0 and residual curvature χ, and the local stress and strain states, i.e. residual stress σ_r and plastic strain ε_p.

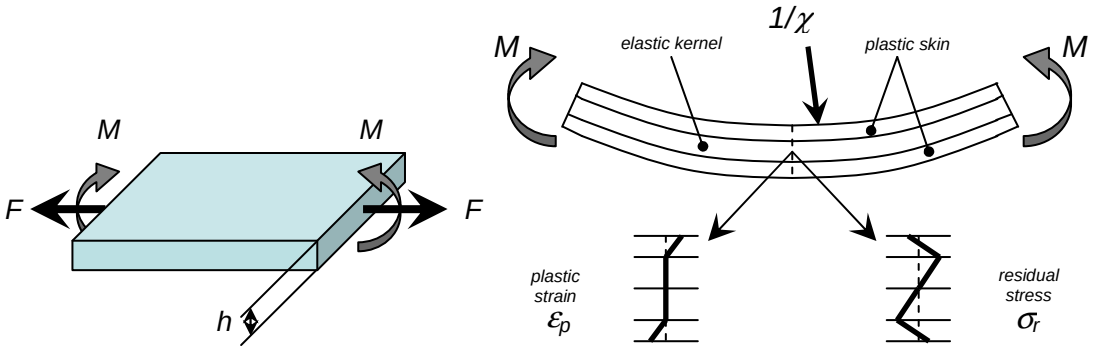

Figure 7. Thin steel sheet subject to elementary deformations and loads: zoom on flexural deformation (right).

The following hypotheses are assumed: homogeneous and isotropic material; plane stress and small strains (i.e. before necking); Von Mises plasticity model; elastic-plastic behaviour: a) without hardening or b) with linear isotropic hardening (see left side of figure 2). All remarks are based on monotonic loading and complete decoupling between thickness variation (membrane deformation) and curvature (flexural deformation), i.e. traction and flexion stress / strain states. Cauchy stress and logarithmic strains are considered.

4.1 Membrane plastic deformation

During membrane deformation, local stress and strain states are uniform through the thickness. Moreover, for isotropic hardening, no residual stress is left in the sheet after plastic deformation. The thickness variation is directly related to the plastic strain tensor and does not depend on the hardening model. Basic solid mechanics and plasticity calculation gives:

$$\varepsilon_p = -B \log\left(\frac{h}{h_0}\right) \approx B\left(1 - \frac{h}{h_0}\right) \tag{2}$$

where ε_p is the Von Mises equivalent plastic strain, h / h_0 the thickness variation and B a coefficient depending on the stretching mode: $B = 2$ for uniaxial tension (TU), $B = 1$ for plane strain tension (TP) and $B = 0.5$ for equi-bi-axial stretching (EB). Equation (2) is plotted in the left side diagram of figure 8.

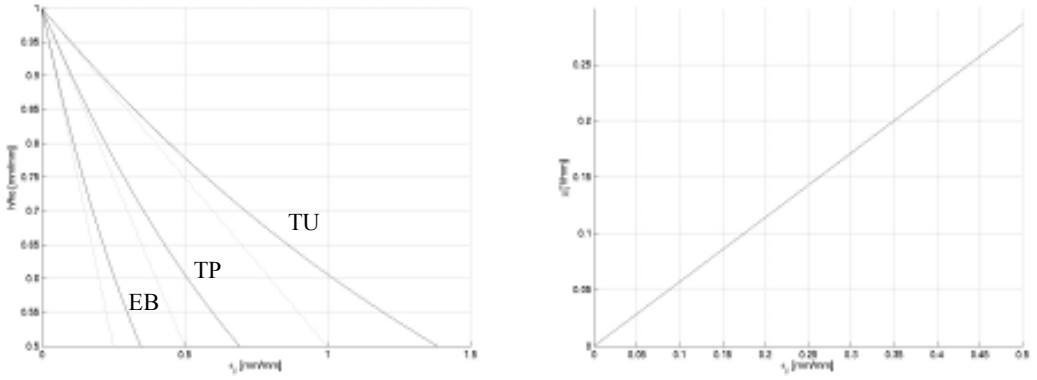

Figure 8. Von Mises equivalent plastic strain related to: thickness variation (equation 2) in membrane plastic deformation (left), residual curvature (equation 3) in flexural plastic deformation (right).

Let us resume the effect of membrane plastic deformation as shown in the left side of figure 9: according to basic solid mechanics, membrane and flexural stresses vary proportionally to $(h / h_0)^{-1}$ and to $(h / h_0)^{-2}$ respectively, while the fatigue limit is supposed to respect equation (1), for which the Von Mises equivalent

plastic strain is calculated via equation (2). Considering A = 1.0 and B = 1.0, the thickness variation has almost the same quantitative effect on the membrane stress and fatigue limit improvement. On the contrary, flexural stress is far more magnified by thickness variation then the fatigue limit.

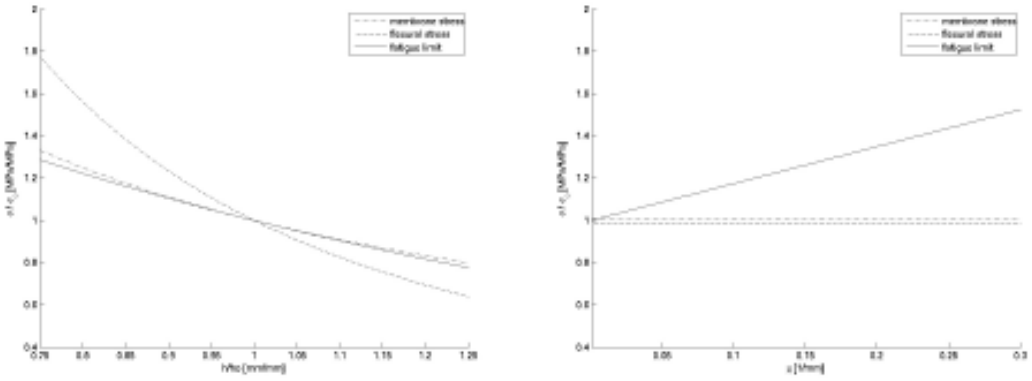

Figure 9. Forming process influence: membrane plastic deformation (left), flexural plastic deformation (right).

4.2 Flexural plastic deformation

In flexural deformation, local stress and strain states vary through the thickness. We assume that every cross section remains plane and normal to the membrane layer, e.g. no shear and warping effects are taken into account. In this framework, all stress and strain are linear and symmetric functions of the local distance from the middle layer (see right side of figure 7). During elastic deformation, maximum stress and strain are located at the external surface (skin). When plasticity occurs, an elastic kernel is surrounded by two plastic skins, so that plastic deformation is always maximum on the skin, while maximum stress is expected to be located at the boundary between the elastic kernel and the plastic skin. Finally, in the isotropic hardening framework, spring-back is supposed to be totally elastic.

The residual sheet curvature, i.e. after spring-back, is directly related to the maximum Von Mises equivalent plastic strain does not strongly depend on the hardening model. Basic solid mechanics and plasticity calculation simply gives:

$$\varepsilon_p \approx \frac{h_0}{2}\,\chi \tag{3}$$

where ε_p is the maximum Von Mises equivalent plastic strain on the sheet skin, h_0 is the nominal sheet thickness and χ the residual curvature after elastic spring-back. Equation (3) is plotted in the right side diagram of figure 8.

Let us resume the effect of membrane plastic deformation as shown in the right side of figure 9: according to basic solid mechanics, membrane and flexural stresses vary proportionally to $(h / h_0)^{-1}$ and to $(h / h_0)^{-2}$ respectively, but in this case no thickness variation is supposed to occur. Meanwhile, the fatigue limit is supposed to respect equation (1), for which the maximum Von Mises equivalent plastic strain is calculated via equation (3). No matter of coefficient A and B values, in perfect flexural plastic deformation the forming process seems just to improve the fatigue limit. Actually, the residual stress is supposed to be taken into account and a framework similar to that of membrane plastic deformation is expected to be found.

5 DISCUSSION AND CONCLUSION

Let us show the qualitative influence of the forming process on the fatigue design, as sketched on the right side of figure 2: in the so-called Dang Van diagram, which represents the mesoscopic shear stress τ as a function of the hydrostatic pressure p, we plot the local stress path (V-shaped solid line) versus the material safety limit (oblique dashed line). From a general point of view, stamping usually decreases thickness: according to basic solid mechanics, this implies that for the same external loading, the local stress path is magnified, as shown by solid arrows, proportionally to $(h / h_0)^{-1}$ for membrane stress and to $(h / h_0)^{-2}$ for flexural stress. Moreover, forming process is supposed to increase strength by work hardening, as represented by the dashed arrow and modelled by equation (1). Finally, possible residual stress, which means nonzero initial hydrostatic pressure, is expected to translate the stress path, as depicted by the dotted arrow.

In a pragmatic approach, strength increase due to work hardening is considered to compensate for thinning and / or to provide an additional safety factor. Moreover, residual stress is simply neglected.

From a "global approach" point of view (section 3), which means the use of coupled process and fatigue FE computation of the entire part, we recover the main conclusions of [3] on a similar chassis part. First of all, we note that the focus area does not change from the initial uncoupled FEA. There, a local thickness reduction of 1.5% implies a safety factor reduction of about the same amount: in this case the local stress path is magnified by $(h / h_0)^{-n}$, with $1<n<2$ as expected for a combined membrane and flexural deformation. Updating local fatigue properties significantly increases the safety factor and seems to largely compensate for thickness reduction, which has to be related to figure 9 abacuses. Finally, residual stress effect is the most dominating and implies a significant evolution of the damage field and a drastic reduction of the safety factor; actually this is found strongly dependent on the choice of the material hardening model. The present case is based on the Dang Van fatigue approach, but it could be extended to any other as far as the forming effects are modelled accordingly.

We remind that such a complete coupled computation is allowed only if a FE forming model is available. In order to overcome this requirement a "local approach" is currently being developed (section 4), based on elementary plastic deformation decomposition. Although curvature computation from CAE membrane design is affordable, the corresponding estimation of the thickness variation is far less straightforward and depends upon the local stretching mode. Actually, the hypothesis on complete decoupling between thickness variation by membrane deformation and curvature by flexural deformation needs to be investigated furthermore.

No matter of the global / local approach, some basic questions still remain unanswered: first of all, the identification of the material constitutive model (isotropic/anisotropic) and hardening model (isotropic/ kinematic) is fundamental prior to any FE computation. Moreover, some numerical details of FEA, such as the choice of a minimum number of integration points within the thickness when considering plasticity in flexural deformation, have to be considered in order to consolidate any numerical computation.

6 REFERENCES

6.1 Books

1. Dang Van K., Macro–micro approach in high-cycle multi-axial fatigue, McDowell DL, Ellis R, editors. Advances in multi-axial fatigue, ASTM STP 1191, Philadelphia, PA: ASTM, 1993, 120–30

6.2 Conference Proceedings

2. B. Yan, P. Belanger, K. Citrin, Effect of forming strain on fatigue performance of a mild automotive steel, SAE world congress, March 5-8, 2001
3. G. Lavinal, C. Laloye, L. Taupin, F. El-Khaldi, C. Lienard, Simulated behaviour of sheet metal chassis parts taking into account the effect of forming, EUROPAM, October 21-22, 2002

6.3 Journal Articles

4. Papadopoulos IV, Fatigue limit of metals under multi-axial stress conditions: the microscopic approach., Technical Note No. I.93.101, Commission of the European Communities, Joint Research Centre, ISEI/IE 2495/93, 1993
5. A. Gustavsson, M. Larsson, A. Melander, Fatigue life of pressed steel components, Int. J. of Fatigue, vol. 19, n. 8-9, 1997, 613-619
6. D. Cornette, A. Galtier, Influence of the forming process on crash and fatigue performance of high strength steels for automotive components, JSAE 2002-02M-57
7. A. Galtier, P. Cugy, E. Marconne, Y. Yoshida, A. Seto, J.-L. Robert, Integration of process operation in the fatigue calculation of sheet structural parts, JSAE 2003-01-2879
8. K. Berchem, M.G. Hocking, The influence of pre-straining on the high-cycle fatigue performance of two hot-dip galvanised car body steels, Material Characterisation, 58, 2007, 593-602

6.4 Dissertations or Thesis

9. C. Doudard, Détermination rapide des propriétés en fatigue à grand nombre de cycles à partir d'essais d'échauffement, PhD thesis, ENS Cachan, 2004

6.5 Commercial codes

10. Abaqus/Standard, v6.5, www.abaqus.com
11. Design Life, ICE-flow v4.1, nCode International Ltd., www.ncode.com
12. Pamstamp 2G, v2005.0.2 ESI group, www.esi-group.com